European Journal of Orthodontics 25 (2003) 109–115

Three-dimensional analysis of endosseous palatal implants and bones after vertical, horizontal, and diagonal force application

T. Gedrange*, C. Bourauel**, C. Köbel* and W. Harzer*
Departments of Orthodontics, *Technical University of Dresden, **University of Bonn, Germany

SUMMARY The effects of bite and orthodontic forces exerted on endosseous palatal implants are not completely understood. This applies especially to the biomechanical properties inherent in the different implant geometries and resulting bone remodelling reactions on the one hand, and to the influence on the direction and magnitude of the applied forces on the other. The results of this study should help in the selection of implants for clinical use.

Three types of endosseous implants (all 9 mm in length and 3.3 mm in diameter, made of titanium) were used for this investigation. Type 1 was a simple, cylinder-shaped implant; type 2 a cylinder-shaped implant with a superperiosteal step; and type 3 a cylinder-shaped implant, subperiosteally threaded, with a superperiosteal step. The load on the implant was investigated under three conditions of bite and orthodontic forces from 0.01 to 100 N (vertically, horizontally, and diagonally). The study results were calculated by means of a finite element (FE) method.

Vertical loading caused bone deformation of more than 600 µeps at the simple implant. The largest deformations at this load were found in the trabecular bone with all three implant geometries. However, trabecular bone deformation was reduced by a superperiosteal step. Horizontal loading of the implants shifted the deformation from the trabecular to the cortical bone. Furthermore, a large deformation was measured at the transition from cortical to trabecular bone. The smallest deformations (less than 300 µeps) were found for implants with a superperiosteal step and diagonal loading (type 2). The use of threads provided no improvement in loading capacity.

All implant types investigated showed good biomechanical properties. However, endosseous implants with a superperiosteal step had the best biomechanical properties under low loads. Thus, the trend should be to optimize the design of implants by producing small implants with additional anchorage on the bone surface.

Introduction

Maximum anchorage or movement of teeth in the posterior direction in order to obtain space is important in orthodontic treatment. This type of treatment often depends on good patient co-operation (Schweizer *et al*., 1996). A compliance-independent alternative is provided by temporary osseointegration of implants in the median palatal suture area (Triaca *et al*., 1992; Wehrbein, 1994; Block and Hoffmann, 1995).

The variety of implant systems for orthodontic anchorage has created confusion because most clinical investigations on direction of force and moments applied have not been well documented. Additionally, changes in implant surfaces and design cause bone remodelling reactions. Bone tissue has been observed on the surface of titanium implants (Piattelli *et al*., 1995). In addition to the implant material, e.g. titanium or aluminium oxide, and the condition of the implant surface, the biomechanical reliability inherent in the different geometries of implants is important (Cook *et al*., 1981; Lavernia *et al*., 1982). The use of implants with a threaded surface is predominant in orthodontic treatment (Wehrbein *et al.*, 1999).

Recent implant developments and studies of mechanical bone stimulation have enabled limits to be defined between physiological and non-physiological transmission of strength to the bone (Joos *et al*., 2000). Biomechanical influences on bone structure play an important role in the longevity of bone around implants (Skalak, 1983). The quantity and direction of force applied influence the implants and cause deformation of the palate suture.

The load transferred from the teeth via the transpalatal arch to the implant during chewing may be as high as 200 N. However, such loading of the tooth–implant complex is of short duration (Skalak, 1983; Paphangkorakit and Osborn, 1998). At such a large load the teeth are connected with bone by the periodontium, whereas the implant is integrated with the bone. These forces by far exceed the levels required for orthodontic anchorage purposes. The anchorage load and occlusal forces are reproduced from the teeth on the implant due to rigid connection of the transpalatal arch. This deformation may cause stress in the bone around the implants and may lead to bone resorption and loss of the implant. Therefore the design of the implant

at relatively low loads up to 100 N determines anchorage stability.

Current research on implants indicates that bone adaptation to implants is an important factor in successful implant treatment. Implant success was defined by Schnitman and Shulman (1979) as mobility of less than 1 mm in any direction. Implants for orthodontic anchorage have a maximum functional service life of 1 year, during which time no mobility should be observed. These guidelines are important because any degree of implant mobility generally indicates impending failure. Stress analyses of different endosseous implants are necessary for the investigation of bone growth and maximum anchorage success. Incorrect loading or overloading as a result of ineffective implant geometries may lead to implant loss and to disturbed bone growth.

The aims of this study were to produce more insight into the influence of the design of an implant system and the direction of force on stress distribution, and to compare the stress patterns of endosseous implants and surrounding bone from the palatal suture area, using the finite element (FE) method. The model was subjected to simulated bite and orthodontic forces of up to 100 N in three different directions. A common implant design with two modifications was used for all load cases.

Material and methods

Dimensions and properties of the implant design

Three-dimensional (3D) models from implants and bone were generated to analyse maximum anchorage load. The maximum principal strain and strain energy density distributions of the implants and bone were evaluated by FE analysis. FE models of the implant–bone complex were generated to determine stresses and strains in the bone adjacent to the implant surface under loading. The results were recorded during static loading in the bone around the implant. The FE method offers various advantages, including accurate representation of complex geometries, easy model modification, and representation of the internal state of stress and other mechanical quantities (Lavernia *et al.*, 1981; Huiskes and Chao, 1983).

Three endosseous implant designs all with a diameter of 3.3 mm and a total length of 9 mm were used for this investigation. Type 1 was a simple, cylinder-shaped implant. The abutments were 3 mm long (Figure 1a). Type 2 was a cylinder-shaped implant with a superperiosteal step on the surface of the compact bone. The subperiosteal part measuring 6 mm in length was identical in shape to type 1. The superperiosteal step in the abutment was 1 mm long and 4 mm in diameter (Figure 1b). Type 3 was a cylinder-shaped implant with a superperiosteal step and a subperiosteal threaded surface. The superperiosteal step in the abutment was 1 mm long and 4 mm in diameter (Figure 1c). The subperiosteal thread had nine steps. The geometries of the three implants were similar to those of commercial implants and all three were made of titanium.

Bone and implant properties

It was important for the experimental model to simulate the original as accurately as possible in anatomical shape and dimension, in physical properties and quantities, and in boundary conditions. Endosseous implants were inserted into the mid-palatal suture of the nasomaxillary complex of three pigs ('Landedelschwein' breed, 12 months old). The palatal suture and the position of the implants were then compared by preparing and analysing non-decalcified microsections of the nasomaxillary complex (Figure 1a–c), following the method of Donath (1992).

The quality and compactness of trabecular and cortical bone in the palatal suture was determined from the histological samples. The bone was also modelled as a heterogeneous beam with realistic cross-sectional dimensions, and cortical and trabecular bone distribution. The 3D FE model had a cortical surface thickness of 2.0 mm for the oral–palatal cortical bone, a trabecular thickness of 5.5 mm, and cortical surface of 1.0 mm in the direction of the nasal floor.

The mechanical characteristics of the palatal suture were obtained from the results of studies from different authors and determined by Young's modulus (E) and Poisson's ratio (ν) (Weinstein *et al.*, 1976; Cook *et al.*, 1981; Lavernia *et al.*, 1982; Borchers and Reichart, 1983; Rieger *et al.*, 1989; Siegele and Soltesz, 1989; van Rossen *et al.*, 1990). In the cortical bone, Young's modulus was assumed to be E = 15 GPa and Poisson's ratio $\nu = 0.33$; in the trabecular bone, values were set to E = 1.5 GPa and $\nu = 0.3$, and for titanium (implant material) the values were taken to be E = 110 GPa and 0.3 ν.

Implant loading

The effects of the three different static loading directions (vertical, horizontal, and diagonal with a 45 degree angle with respect to the implant axis) on three types of implants were examined. The load on the upper part of implant abutments was investigated under potential bite and orthodontic forces ranging from 0.01 to 100 N. The load on the bone was determined in graduations of 10, 30, and 70 N.

FE method

Stresses and strains in the implant, the bone, and the bone–implant interface were calculated by FE analysis. The FE method is a numerical method of engineering mechanics, where the structure to be investigated is discretized into a certain finite number of elements. The

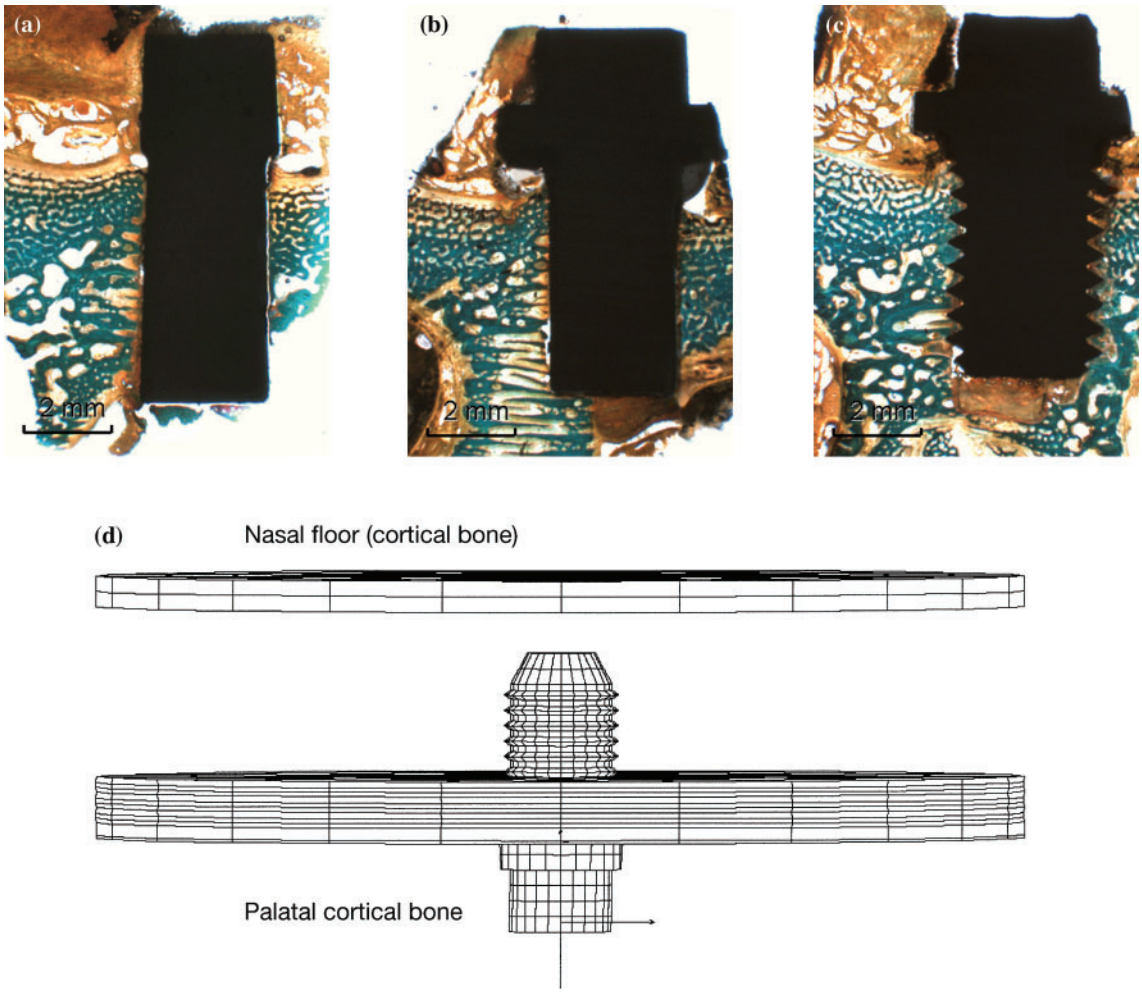

Figure 1 Undecalcified cross-sections of palatal bone with implant. Goldner-reaction staining. Histological investigations of quality and quantity of different bone structures in the palatal suture of pigs. (a) Implant type 1 (simple, cylinder-shaped); (b) implant type 2 (cylinder-shaped implant with superperiosteal step); (c) implant type 3 (cylinder-shaped implant, subperiosteally threaded with superperiosteal step). (d) Finite element model of implant type 3. The implant is inserted into the palatal cortical and the spongious bone. The latter was removed from the model to make the implant thread visible.

mechanical behaviour of each element is described by a set of differential equations that can be solved with the aid of a computer program. Based on the material parameters and the forces applied, it is possible to determine the mechanical stresses and strains, as well as the deformations of the individual components of the model, i.e. implant, cortical bone, spongious bone, and the whole structure (Bathe, 1986). Figure 1d shows the FE model of the threaded implant with the surrounding bone structure. The spongious bone was removed from the model to make the implant thread visible. The deformation of implant geometry and palatal suture region was investigated. The study was performed using the commercial FE package COSMOS/M 2.5, running on an Athlon-850 PC under Windows NT. The eight-noded solid volume element was used employing the geometrically non-linear option.

Data representation focuses on discussion of the strains in the bone. A current measure for small strain values is μstrain or μeps, where a strain of 1 means a deformation of 100 per cent. Thus, for example, a strain of 100 μeps coincides with a strain of 0.0001 or 0.01 per cent ($\mu = 10^{-6}$). The determination of mechanical bone damage and fatigue was carried out according to Frost (1994).

Results

Implant deformation

No damage was registered in the investigated implants under the three conditions of bite and orthodontic forces with loading up to 100 N. Implant deformation was minimal and similar in all implants. The maximum strain on the implant was less than 0.01 per cent.

Peri-implant bone deformation during loading

A linear correlation between bone deformation and implant load was determined. The changes were calculated from 0 N, and deformations from 0 μeps up to a static load of 100 N. For improved clarity, the bone deformation is represented only at 100 N in the figures. The same type of deformation was seen at all other load units under 100 N.

The subperiosteal component was equally long in all implants. A finer division was chosen for the subperiosteally threaded implant, so that more *Z*-co-ordinates were indicated. For the simple implant and the implant with a superperiosteal step, the results were determined at the top edges of the FE, so that the co-ordinate of the bottom edge of the implant is missing. Consequently, values are reported for a depth of 5.5 mm in Figures 2–4.

Vertical loading

The calculated bone strains up to a load of 100 N are shown in Figure 2a, b, and c. The load in the cortical bone was concentrated at the neck of the implant with the simple implant having a 6-mm subperiosteal component.

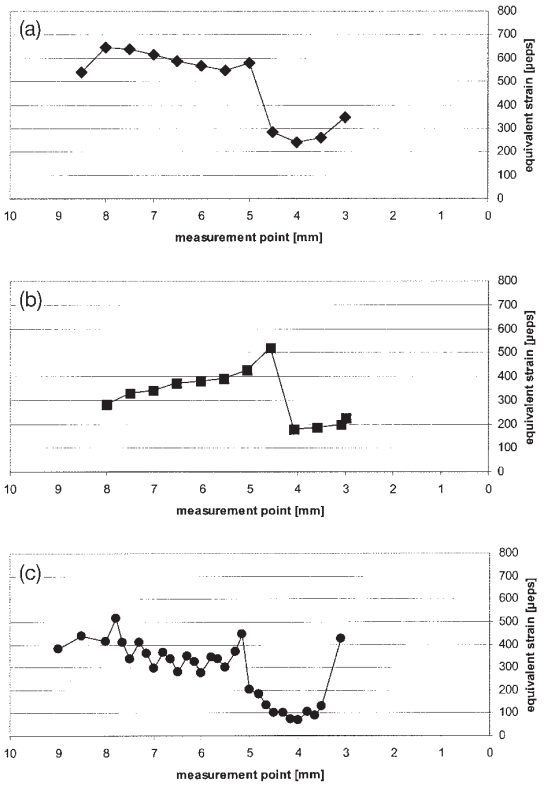

Figure 2 Strain distribution in bone–implant complex under vertical loading at a force of up to 100 N. Overall implant length = 9 mm. (a) Implant type 1 (simple, cylinder-shaped); (b) implant type 2 (cylinder-shaped implant with superperiosteal step); (c) implant type 3 (cylinder-shaped implant, subperiosteally threaded with superperiosteal step).

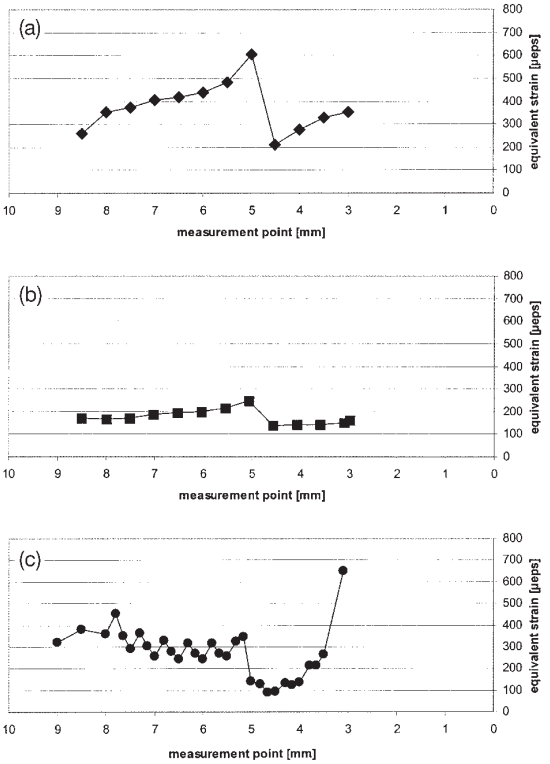

Figure 3 Strain distribution in bone–implant complex under diagonal loading at a force of up to 100 N. Overall implant length = 9 mm. (a) Implant type 1 (simple, cylinder-shaped); (b) implant type 2 (cylinder-shaped implant with superperiosteal step); (c) implant type 3 (cylinder-shaped implant, subperiosteally threaded with superperiosteal step).

The load on the implant caused a deformation in the cortical bone of approximately 300 μeps. The deformations doubled in the area of trabecular bone and remained almost unchanged at the apex of the implant. The deformations up to 650 μeps represent the highest level recorded in the trabecular bone.

With the superperiosteal step there was a reduction in bone deformation. There was an approximately 30 per cent lower deformation of the cortical bone under load for the simple implant (6-mm subperiosteal component) with a superperiosteal step in comparison with those with no superperiosteal step. The largest deformation was measured at the transition from cortical to trabecular bone. The deformation underwent a continuous decrease towards the apex.

For the implant with a superperiosteal step and subperiosteally threaded component, heterogeneous bone deformation was caused by the thread on the implant surface. The very strong deformation of the surface of the cortical bone in the upper part of the implant–bone complex decreased by one-quarter at a cortical depth of 0.4 mm to approximately 100 μeps. The increase in bone deformation recorded at the transition from cortical to trabecular bone was less pronounced than with all other implants. The strain increased towards the apex.

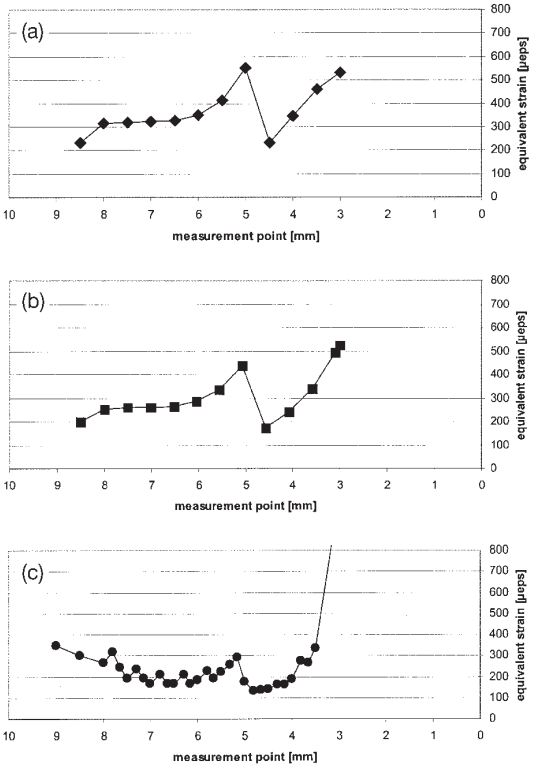

Figure 4 Strain distribution in bone–implant complex under horizontal loading at a force of up to 100 N. Overall implant length = 9 mm. (a) Implant type 1 (simple, cylinder-shaped); (b) implant type 2 (cylinder-shaped implant with superperiosteal step); (c) implant type 3 (cylinder-shaped implant, subperiosteally threaded with superperiosteal step).

Diagonal loading

The bone strains recorded at 100 N are shown in Figure 3a, b, and c.

The deformation of the cortical bone decreased from the bone surface to the trabecular bone by one-third to a value of 200 µeps. The deformation increased immediately in the trabecular bone to 600 µeps and decreased at the apex, so that similar results were found.

The lowest bone deformations were determined at an oblique load on the implant with a superperiosteal step. After low deformation of the cortical bone, almost 250 µeps were reached at the transition from cortical to trabecular bone.

The largest surface deformations of the cortical bone were registered on loading the implant with a superperiosteal step and subperiosteal thread. The results showed a 50 per cent increase in this area in comparison with the other implants. The deeper regions of the cortical bone (1.4 mm) showed only one-seventh of the surface deformation of cortical bone. The area of trabecular bone and apex showed a similar deformation to simple implants.

Horizontal loading

The registered bone strains at 100 N are displayed in Figure 4a–c.

The largest deformations in cortical bone were caused by loading the simple implant with horizontal forces. The deformation decreased sharply in deeper regions of the cortical bone. In the upper region of the trabecular bone the deformation was the same as in the upper region of the cortical bone. The deformation of the trabecular bone decreased towards the apex, so that the results were equivalent to those in the deeper regions of the cortical bone (cortical bone 232 µeps, apex 233 µeps).

The implant with one superperiosteal step caused a similar bone deformation. However, this deformation was smaller compared with the simple implants. The same deformation was recorded only in cortical bone.

Under horizontal loading, the implant with the superperiosteal step and thread showed the largest deformations of cortical bone compared with all implant designs and loads. However, the deeper regions of the cortical bone showed very small deformations, which were even smaller than those registered with simple implants and in implants with a superperiosteal step. The deformations increased slightly in the area of the trabecular bone, but the strains were lower than those of the two other implant designs.

Discussion

The aim of the present study was to investigate the deformation of the bone surface around an implant in response to different force magnitudes and different directions of force application. Bone tissue is known to remodel its structure in response to mechanical stress. Low stress levels around an implant may result in poor connection with bone or bone atrophy (Meijer *et al.*, 1993). On the other hand, abnormally high stress concentrations in the supporting tissues can result in pressure necrosis and subsequently in implant failure (Lavernia *et al.*, 1981).

The palatal suture of the pig is similar to that of humans and is particularly suitable for investigations with regard to anatomical structure and deformation under stress (Weaver *et al.*, 1962; Gedrange *et al.*, 2001). The FE method was adapted largely to clinical conditions by selecting parameters such as implant and bone shape, stress, and its direction. By applying the FE method, the influence of different implant designs and direction of the force on palatal bone was observed. Comparing qualitative results for three different implant geometries revealed that during force application the critical region is the transition from cortical to trabecular bone.

The results of studies of dental implants (Rieger *et al.*, 1990; Joos *et al.*, 2000; Meyer *et al.*, 2001) using FE analysis can be compared with the quantitative results

obtained in the present analysis. The simple orthodontic implant caused the highest strains in the trabecular bone. The strain distribution from the trabecular bone to the neck of the implant could be decreased by changing the implant design. By adding a superperiosteal step to the implants the highest strains were registered around the neck position. The step improved the stability of the implant–bone complex. The best results were achieved by increasing the implant surface by means of a screw thread.

Analysis of the implant with a superperiosteal step after diagonal loading showed that the two strain regions at the neck and apex of the implant consisted of vertical compressive strains and upward orientated strains on the implants without important horizontal strain components. The actual magnitudes of strain can cause bone remodelling. It has been suggested in the literature that there is an optimal value of strain which causes remodelling by bone resorption. Van Rossen *et al.* (1990), Holmes *et al.* (1992), and Kregzde (1993) reported similar values for maximum equivalent strains in cortical and trabecular bone around a free-standing implant.

A large strain was found in the cortical bone for all the investigated implant designs under three types of load. The strain in the diagonal direction was smaller than in the horizontal and vertical directions. To reduce high loading peaks, attention must be paid to the direction of chewing and bite force, as these variables have more influence than the connection of the implants to bone. The direction of the chewing force cannot be varied in patients, but the magnitude can be influenced by the design of the implant and by its position in the palate (Meijer *et al.*, 1993). The anchorage load and occlusal forces are transmitted from the teeth onto the implant due to rigid connection of the transpalatal arch. The implant transmits the load to the bone tissue and palatal vault.

Essential bone features underlying biological growth processes were not included in this FE model. Sustained under- or over-strain leads to a change in biomechanical bone features, resulting in insufficient vascularization.

The simulation showed that the degrees of ossification of trabecular and cortical bone depend essentially on the selected load limit (Frost, 1994) as underloading results in no changes, and overloading to bone fracture. The maturation process runs asymptotically into a stable configuration characterized by incomplete ossification.

Models reflecting the true situation were used as far as possible, but the simulation of heterogeneity and anisotropy of bone and properties of implant surface must be considered in future clinical studies.

Conclusions

The results suggest that implant geometries can provide adequate orthodontic anchorage subject to modification of force stress. However, the design must not cause high stress concentrations at the implant neck, as these commonly cause bone resorption.

The use of a strain energy density criterion as the objective function proved to be the most effective in reducing all equivalent stress criteria.

The best result of the FE investigation was recorded at implants with a superperiosteal step and under diagonal loading. This implant geometry and type of load may permit the implant–bone complex to be stressed immediately after implantation.

The use of threads provided no improvement in load capacity. Thus, the aim of all designs should be to produce a relatively small implant with a screw thread cross-section and superperiosteal step at the bone surface.

Address for correspondence

Dr T. Gedrange
Poliklinik für Kieferorthopädie
Universitätsklinikum TU Dresden
Fetscherstr. 74
D-01307 Dresden
Germany

References

Bathe K J 1986 Finite-Elemente-Methoden. Springer, Berlin

Block M S, Hoffman D R 1995 A new device for absolute anchorage for orthodontics. American Journal of Orthodontics and Dentofacial Orthopedics 107: 251–258

Borchers L, Reichart P 1983 Three-dimensional stress distribution around a dental implant at different stages of interface development. Journal of Dental Research 62: 155–159

Cook S D, Klawitter J J, Weinstein A M 1981 The influence of implant elastic modulus on the stress distribution around LTI carbon and aluminum oxide dental implants. Journal of Biomedical Materials Research 15: 879–887

Donath K 1992 Pathogenesis of bony pocket formation around dental implants. Journal of the Dental Association of South Africa 47: 204–208

Frost H M 1994 Wolff's Law and bone's structural adaptations to mechanical usage: an overview for clinicians. Angle Orthodontist 64:175–88

Gedrange T, Köbel C, Harzer W 2001 Hard palate deformation in an animal model following quasi-static loading to stimulate that of orthodontic anchorage implants. European Journal of Orthodontics 23: 349–354

Holmes D C, Grigsby W R, Goel V K, Keller J C 1992 Comparison of stress transmission in the IMZ implant system with polyoxymethylene or titanium intramobile element: a finite element stress analysis. International Journal of Oral & Maxillofacial Implants 7: 450–458

Huiskes R, Chao E Y 1983 A survey of finite element analysis in orthopedic biomechanics: the first decade. Journal of Biomechanics 16: 385–409

Joos U, Vollmer D, Kleinheinz J 2000 Einfluss der Implantatgeometrie auf die Strain-verteilung im periimplantären Knochen. Mund-, Kiefer- und Gesichtschirurgie 4: 143–147

Kregzde M 1993 A method of selecting the best implant prosthesis design option using three-dimensional finite element analysis. International Journal of Oral & Maxillofacial Implants 8: 662–673

Lavernia C J, Cook S D, Weinstein A M, Klawitter J J 1981 An analysis of stresses in a dental implant system. Journal of Biomechanics 14: 555–560

Lavernia C J, Cook S D, Weinstein A M, Klawitter J J 1982 The influence of the bone–implant interface stiffness on stress profiles surrounding Al2O3 and carbon dental implants. Annals of Biomedical Engineering 10: 129–138

Meijer H J, Steen W H, Bosman F 1993 A comparison of methods to assess marginal bone height around endosseous implants. Journal of Clinical Periodontology 20: 250–253

Meyer U, Vollmer D, Runte C, Bourauel C, Joos U 2001 Bone loading pattern around implants in average and atrophic edentulous maxillae: a finite-element analysis. Journal of Cranio-Maxillofacial Surgery 29: 100–105

Paphangkorakit J, Osborn J W 1998 Effects on human maximum bite force of biting on a softer or harder object. Archives of Oral Biology 43: 833–839

Piattelli A, Scarano A, Piattelli M 1995 Detection of alkaline and acid phosphatases around titanium implants: a light microscopical and histochemical study in rabbits. Biomaterials 16: 1333–1338

Rieger M R, Fareed K, Adams W K, Tanquist R A 1989 Bone stress distribution for three endosseous implants. Journal of Prosthetic Dentistry 61: 223–228

Rieger M R, Mayberry M, Brose M O 1990 Finite element analysis of six endosseous implants. Journal of Prosthetic Dentistry 63: 671–676

Schnitman P A, Shulman L B 1979 Recommendations of the consensus development conference on dental implants. Journal of the American Dental Association 98: 373–377

Schweizer C M, Schlegel K A, Rudzki-Janson I 1996 Endosseous dental implants in orthodontic therapy. International Dental Journal 46: 61–68

Siegele D, Soltesz U 1989 Numerical investigations of the influence of implant shape on stress distribution in the jaw bone. International Journal of Oral & Maxillofacial Implants 4: 333–340

Skalak R 1983 Biomechanical considerations in osseointegrated prostheses. Journal of Prosthetic Dentistry 49: 843–848

Triaca A, Antonini M, Wintermantel E 1992 Ein neues Titan-Flachschrauben-Implantat zur orthodontischen Verankerung am anterioren Gaumen. Informationen aus Orthodontie und Kieferorthopädie 24: 251–257

Van Rossen I P, Braak L H, De Putter C, De Groot K 1990 Stress-absorbing elements in dental implants. Journal of Prosthetic Dentistry 64: 198–205

Weaver M E, Sorenson F M, Jump E B 1962 The miniature pig as an experimental animal in dental reserch. Archives of Oral Biology 7: 17–24.

Wehrbein H 1994 Enossale Titanimplantate als orthodontische Verankerungselemente. Fortschritte der Kieferorthopädie 55: 236–250

Wehrbein H, Yildirim M, Diedrich P 1999 Osteodynamics around orthodontically loaded short maxillary implants. An experimental pilot study. Journal of Orofacial Orthopedics 60: 409–415

Weinstein A M, Klawitter J J, Anand S C, Schuessler R 1976 Stress analysis of porous rooted dental implants. Journal of Dental Research 55: 772–777